

## Fully differential cusp electron production cross sections for 75-keV $\text{H}_2^+$ +He collisions

L. An, Kh. Khayyat, and M. Schulz

*Physics Department, University of Missouri–Rolla, Rolla, Missouri 65409*

(Received 28 September 2000; published 12 February 2001)

A kinematically complete experiment on single ionization for 75-keV  $\text{H}_2^+$ +He collisions was performed by measuring the fully momentum analyzed projectiles and recoil ions in coincidence. The electron momentum was deduced from momentum conservation. Clear signatures of the postcollision interaction between the outgoing projectiles and the electrons were observed in the momentum spectra of all collision products simultaneously.

DOI: 10.1103/PhysRevA.63.030703

PACS number(s): 34.50.Fa, 34.50.Bw

The fundamental processes occurring in ion-atom collisions are ionization, excitation, and electron capture. In spite of extensive studies over many decades our understanding of these processes is still incomplete. The basic underlying difficulty is that even the most simple collision systems represent at least three-body systems (two nuclei and one electron) for which the Schrödinger equation is not solvable in closed form. A further complication is caused by the long-range nature of the Coulomb force. As a result all the collision products interact with each other at all distances and thus the transition amplitudes in principle involve integration over infinite space.

For ionization processes the interaction between the ionized electron and the projectile after the collision, usually referred to as the postcollision interaction (PCI), is particularly important. For excitation and capture, the electron remains with one of the collision partners and therefore for this interaction the integration can to a good approximation be limited to finite space. For ionization, in contrast, the electron and projectile can depart from each other to large distances. Since the Coulomb force between them vanishes only asymptotically at infinite distance, here effects due to the PCI have to be accounted for over very large spatial dimensions.

For electron emission angles near  $0^\circ$  the PCI between the projectile and the electron leads to a pronounced structure in the ionized electron-energy spectra, which is known as the cusp peak. It represents electrons moving at velocities equal to the projectile velocity. Although cusp electrons are of great importance for emission angles close to  $0^\circ$ , their contribution to the cross sections integrated over all electron angles was assumed to be negligible [1,2].

More recently, effects of the PCI were also observed in the projectile spectra [3,4]. In that experiment the doubly differential cross sections were measured as a function of the projectile scattering angle and the emitted electron energy. Two surprising results were obtained: first, the angular distribution of the projectiles is significantly affected by the postcollisional attraction with the electron. In the width of this distribution as a function of electron energy a minimum was observed at the cusp energy. Previously this was not expected because of the large projectile-to-electron mass ratio. Second, even in the singly differential cross sections effects due to the PCI are not negligible, although the cross sections were integrated over the projectile scattering angle

and the electron emission angle, in contrast to conclusions drawn from previous studies of the ionized electron spectra [5–9].

In order to obtain a complete picture of the mechanism leading to the production of cusp electrons it is also important to obtain detailed information about the recoiling target ions. To this end a major breakthrough was accomplished with the development of recoil ion momentum spectroscopy. It has been demonstrated in numerous papers (for a review see Ref. [10]) that the recoil ion momentum distributions contain detailed information about the dynamics of the single ionization mechanisms. Weber *et al.* reported [11] on an abrupt rise of the longitudinal recoil-ion momentum distributions in proton-helium collisions that was associated with cusp electron production. More recently, kinematically complete experiments were performed by measuring the fully momentum analyzed recoil ions and ionized electrons in coincidence [12–14]. Clear signatures of the PCI were identified both in the recoil ions and electron spectra. However, in these studies only electron energies much smaller than the cusp energy were analyzed. On the other hand, it is known that effects due to the PCI maximize around the cusp energy.

In this work, we report on a kinematically complete study on the production of cusp electrons. A kinematically complete experiment requires determining the momentum vectors of all collision products simultaneously. Single ionization involves three independently moving particles in the final state. Therefore the momentum vectors of two particles have to be measured directly. The momentum vector of the third particle can then be deduced from momentum conservation. We chose to measure the momentum vectors of the projectile and the recoil ion, and the electron momentum was determined from momentum conservation.

The experiment was performed at the University of Missouri–Rolla Ion Energy Loss Spectrometer (IELS). An  $\text{H}_2^+$  beam was produced from a hot cathode ion source with a very narrow energy spread ( $<1$  eV) and accelerated to an energy of 75 keV. The beam intersected with a very cold ( $<1$  K) neutral helium beam from a supersonic gas jet. Two sets of collimators before and after the target chamber defined the polar and azimuthal scattering angles of the projectiles. A switching magnet located after the target chamber separated the different charge states of the projectile. The  $\text{H}_2^+$  ions were then decelerated to an energy of 2 keV and energy-analyzed by an electrostatic parallel plate analyzer,

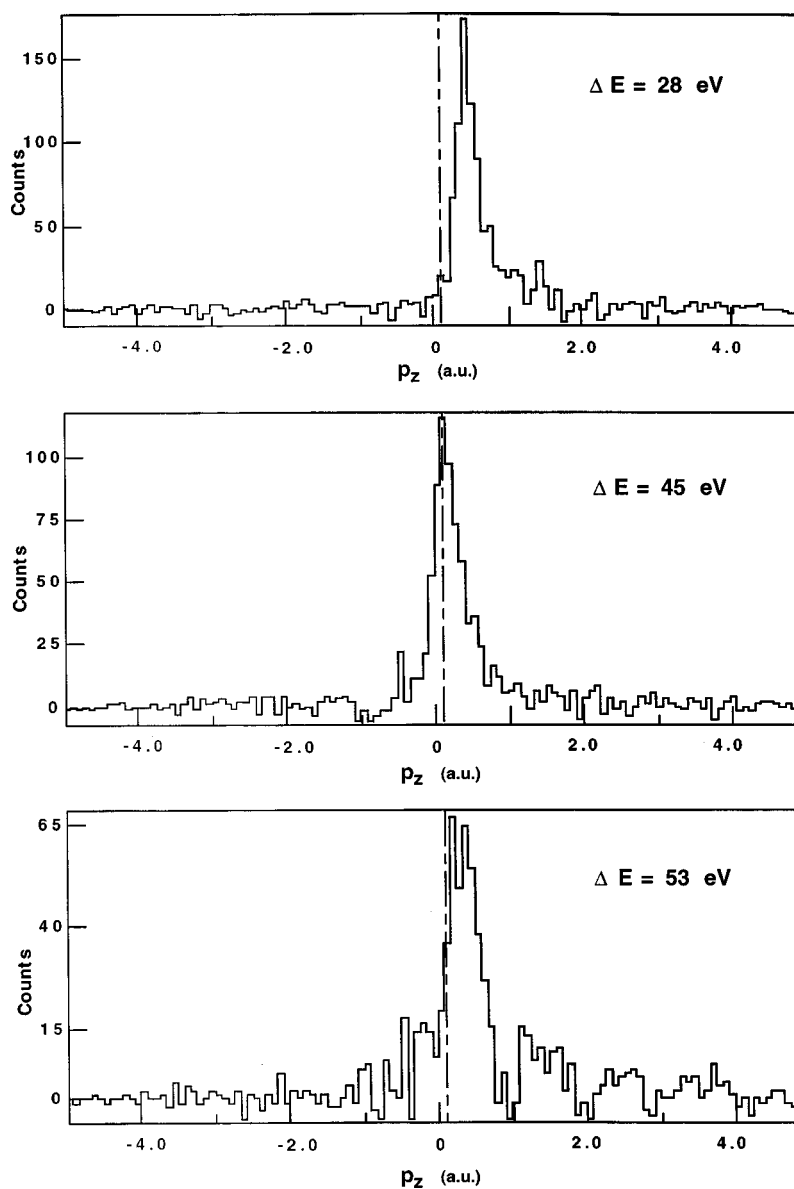


FIG. 1. Recoil ion longitudinal momentum distributions for three different projectile energy losses, 28, 45, and 53 eV, at a zero projectile scattering angle. The dashed line represents the theoretical value for the minimum longitudinal recoil ion momentum  $P_{\parallel}^{\text{min}}$  obtained from Eq. (1).

thus providing the magnitude of the projectile momentum vector. The energy-loss resolution was 1.2 eV full width at half maximum (FWHM) corresponding to a momentum resolution of 0.04 a.u. From the scattering angle the direction of the projectile momentum vector was obtained. The scattering angles were scanned by pivoting the accelerator around the target chamber center. The angular resolution was measured for the incident beam (zero energy loss) to be 0.15 mrad FWHM.

The recoil ions were extracted from the collision region by a weak electric field (2 V/cm) and detected by a two-dimensional position-sensitive detector. From the position information the two momentum components in the plane perpendicular to the extraction field (i.e., the longitudinal component and one of the two transverse momentum components) were obtained. The projectile and the recoil ion

were detected in coincidence. From the coincidence time the time of flight of the recoil ions was deduced, which, in turn, provides the second transverse momentum component. A recoil ion momentum resolution of better than 0.2 a.u. was achieved. More details on the cold target recoil ion momentum spectroscopy (COLTRIMS) method are found in [10]. Momentum and energy conservation is then applied to calculate the electron momentum.

Figure 1 shows the recoil ion longitudinal momentum distributions for three different projectile energy losses. The medium energy loss (45 eV) corresponds to electrons moving at the same speed as the projectile, while the smaller (28 eV) and larger (53 eV) energy losses correspond to slower and faster electrons, respectively. As the figure shows the momentum distributions are very narrow. The FWHM of the peaks lies in the range 0.2–0.3 a.u. (FWHM) depending on

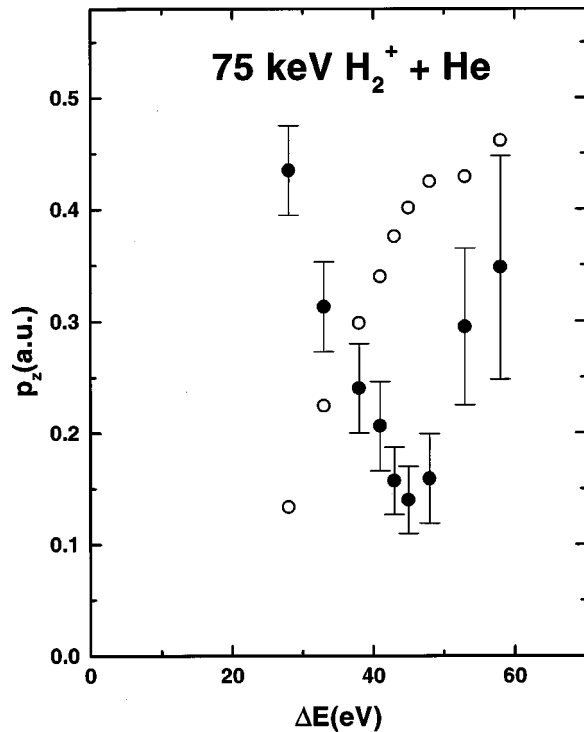


FIG. 2. Centroids of the longitudinal momentum distributions of the recoil ions (closed symbols) and electrons (open symbols) as a function of the projectile energy loss.

the projectile energy loss, which is not much wider than the experimental resolution ( $<0.2$  a.u.). The noncoincident longitudinal recoil ion momentum distribution, in contrast, is significantly wider ( $\sim 0.6$  a.u.).

From energy and momentum conservation it can be shown that there is a minimum recoil ion momentum  $P_{r\parallel}^{\min}$  in the longitudinal direction [15]. This minimum value is given by

$$P_{r\parallel}^{\min} = \frac{I}{\nu_p} - \frac{\nu_p}{2} \quad (1)$$

where  $I$  is the ionization potential of the target atom and  $\nu_p$  is the initial projectile speed. For the collision system studied in this work  $P_{r\parallel}^{\min} = 0.12$  a.u., which is indicated by the dashed line in Fig. 1.

If the peak positions are compared with each other and with the calculated  $P_{r\parallel}^{\min}$ , it is noticed that the momentum distribution peak for the projectile energy loss of 28 eV has a significantly larger value than  $P_{r\parallel}^{\min}$ . As larger energy losses are considered the momentum distribution peak shifts towards smaller values until it almost reaches  $P_{r\parallel}^{\min}$  at an energy loss of 45 eV. Increasing the energy loss further (53 eV) shifts the peak back towards higher values again. To study this shift of the recoil ion longitudinal momentum distribution more systematically, the centroids of the distributions were determined as a function of the projectile energy loss and are plotted in Fig. 2 (closed symbols). A pronounced minimum in the recoil ion longitudinal momentum appears at an energy loss of 45 eV. This minimum occurs at

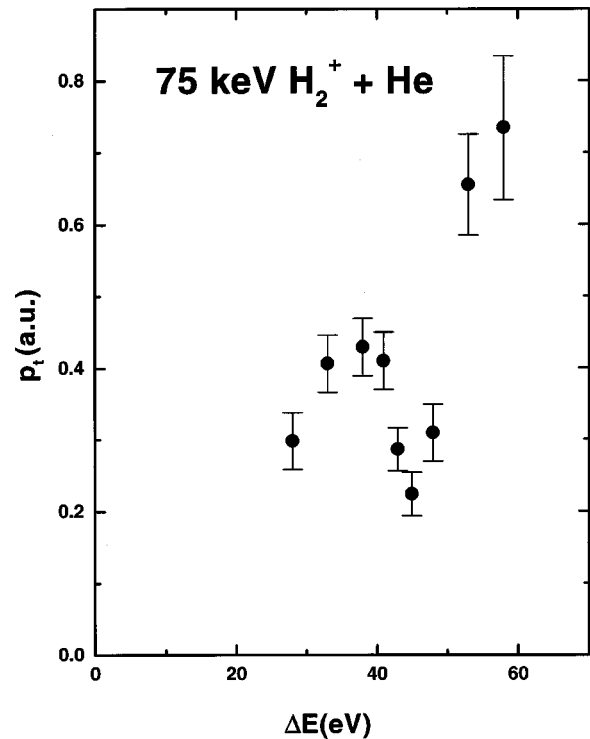


FIG. 3. Centroids of the electron transverse momentum distribution as a function of the projectile energy loss.

a momentum close to  $P_{r\parallel}^{\min}$  obtained from Eq. (1). Furthermore, we note that from kinematics it can be shown that  $P_{r\parallel}^{\min}$  is reached exactly when the longitudinal electron momentum component is equal to the speed of the projectile (matching velocity) [15]. At the same time from the energy loss it is clear that the magnitude of the complete electron velocity vector is also equal to the projectile speed. Combining these observations leads to the conclusion that for an energy loss of 45 eV most electrons have a very small transverse momentum component, i.e., they move at the same velocity vector as the projectiles. Therefore, the minimum in Fig. 2 is a clear signature of cusp electrons.

Since the experiment is kinematically complete, the longitudinal electron momentum can be deduced from the recoil ion momentum and momentum and energy conservation. Figure 2 shows the dependence of the centroid of the longitudinal electron momentum as a function of the projectile energy loss (open symbols). Here the centroids shift almost linearly to larger momenta with increasing energy loss up to the value corresponding to the matching velocity. There the slope changes significantly, leading to an almost flat energy-loss dependence. This shows that increasing the energy transfer to the electron beyond the cusp energy does not significantly increase the longitudinal electron momentum. The electron “prefers” to maintain a longitudinal momentum equal to the projectile speed, which is another signature of the PCI. Therefore, the energy transfer now has to go predominantly into the transverse motion of the electron.

To study the energy transfer to the transverse motion of the electron in more detail the transverse electron momentum distribution was determined using energy and momentum

conservation. The electron kinetic energy, given by  $\Delta E - I$ , can be expressed in terms of the longitudinal and transverse momentum by

$$K_e = \frac{P_{\parallel}^2 + P_{\perp}^2}{2m_e}, \quad (2)$$

so that

$$P_{\perp} = \sqrt{(\Delta E - I)2m_e - P_{\parallel}^2}. \quad (3)$$

It should be noted that, since the data are taken at zero projectile scattering angles, the electron transverse momentum is compensated by the one of the recoil ion; i.e., the recoil ions and the electrons move opposite to each other in the transverse direction.

In Fig. 3 the centroids of the electron transverse momentum distribution are plotted as a function of the projectile energy loss. The figure shows that for small energy losses the transverse momentum increases as the projectile energy loss increases, which is kinematically expected for a symmetric longitudinal momentum distribution [see Eq. (3)]. As the energy loss increases a sudden drop in the momentum distribution occurs at an energy loss of 45 eV. As the energy loss is increased further the centroids shift to larger momenta again.

This supports our above conclusion drawn from the lon-

gitudinal momentum distributions: At the cusp energy very little energy is transferred to the electron in the transverse direction. However, above the cusp energy the transverse momentum increases steeply while the longitudinal momentum remains nearly constant. This can be interpreted as a focusing effect: the attractive PCI focuses the electrons toward the projectile beam axis. This focusing effect maximizes for cusp electrons leading to the minimum at the matching velocity. Our transverse momentum distribution of the electrons, which because of momentum conservation has to be identical to the one for the recoil ions, is significantly different from the one reported by Weber *et al.* [11]. It should be noted, however, that in our work the projectile velocity is significantly smaller. More importantly, in the work of Weber *et al.* the cross sections were integrated over all projectile scattering angles, while our experiment was performed for a fixed scattering angle of  $0^\circ$ .

In summary, we have performed a kinematically complete study on the production of cusp electrons. We thus obtained a comprehensive picture showing the effects of the PCI on the momentum distributions of all collision products simultaneously. Especially in the transverse electron momentum distributions were strong focusing effects observed.

This work was supported by the National Science Foundation under Grant No. PHY 9732150.

- 
- [1] G. B. Crooks and M. E. Rudd, Phys. Rev. Lett. **25**, 1599 (1970).
- [2] K. G. Harrison and M. W. Lucas, Phys. Lett. **33A**, 142 (1970).
- [3] T. Vajnai, A. D. Gaus, J. A. Brand, W. Htwe, D. H. Madison, R. E. Olson, J. L. Peacher, and M. Schulz, Phys. Rev. Lett. **74**, 3588 (1995).
- [4] T. Vajnai, A. D. Gaus, W. Htwe, D. H. Madison, and R. E. Olson, Phys. Rev. A **54**, 2951 (1996).
- [5] M. E. Rudd and D. H. Madison, Phys. Rev. A **14**, 128 (1976).
- [6] W. Meckbach, S. Suárez, P. Focke, and G. Bernardi, J. Phys. B **24**, 3763 (1991).
- [7] R. D. DuBois, Phys. Rev. A **48**, 1123 (1993).
- [8] L. Sarkadi, J. Pálinkás, Á. Kövér, D. Berényi, and T. Vajnai, Phys. Rev. Lett. **62**, 527 (1989).
- [9] S. Suárez, C. Garibotti, W. Meckbach, and G. Bernardi, Phys. Rev. Lett. **70**, 418 (1993).
- [10] J. Ullrich, R. Moshhammer, R. Dörner, O. Jagutzki, V. Mergel, H. Schmidt-Böcking, and L. Spielberger, J. Phys. B **30**, 2917 (1997).
- [11] T. Weber, Kh. Khayyat, R. Dörner, V. D. Rodriguez, V. Mergel, O. Jagutzki, L. Schmidt, K. A. Müller, F. Afaneh, A. Gonzalez, and H. Schmidt-Böcking, Phys. Rev. Lett. **86**, 224 (2001).
- [12] R. Moshhammer, J. Ullrich, M. Unverzagt, W. Schmitt, P. Jardin, R. E. Olson, R. Dörner, V. Mergel, and H. Schmidt-Böcking, Phys. Rev. Lett. **73**, 3371 (1994).
- [13] R. Moshhammer, P. D. Fainstein, M. Schulz, W. Schmitt, H. Kollmus, R. Mann, S. Hagmann, R. E. Olson, and J. Ullrich, Phys. Rev. Lett. **83**, 4721 (1999).
- [14] R. Moshhammer, J. Ullrich, H. Kollmus, W. Schmitt, M. Unverzagt, H. Schmidt-Böcking, C. J. Wood, and R. E. Olson, Phys. Rev. A **56**, 1351 (1997).
- [15] V. D. Rodríguez, Y. D. Wang, and C. D. Lin, Phys. Rev. A **52**, R9 (1995).